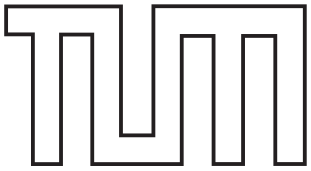

Technische Universität
München

Fachgebiet
Höchstfrequenztechnik

Bachelor's Thesis

77 GHz Automotive Radar Transponder

Author:	Stefan Ries
Matriculation number:	3600268
Advisor:	Dipl.-Ing. Malek Chaabane
Validator:	Prof. Dr.-Ing. Erwin Biebl
Date:	November 1, 2011

Acknowledgment

I hereby confirm that this thesis was written all by myself and all intellectual property of other literature is indicated in the references section.

I sincerely would like to thank Prof. Dr.-Ing. Erwin Biebl for offering me this great project.

Special thanks to my advisor, Dipl.-Ing. Malek Chaabane, for all advices, great promotion on my work and the assistance during the manufacturing process.

The staff of Fachgebiet Höchstfrequenztechnik at TU München, always behaved supportive and gave me great backing during my thesis. Thank you for your input at any time: M.Sc. Martin Blesinger, M.Sc. Gerrit Kalverkamp, Dipl.-Ing. Carolin Loibl, Dipl-Ing. Thomas Reichenthalhammer, Dipl-Ing. Bernhard Schaffer, Dipl-Ing. Florian Pfeiffer Finally, thank you Jana Mögel, for the organization assistance.

Abstract

77 GHz automotive radar transponder - design and construction

In this thesis, a 77 GHz automotive radar transponder will be designed and constructed. Purposes for this are better objective detection and identification in road traffic. It is intended to improve present driving assistance systems, like ACC[1].
This will be achieved through a passive RF[2] transponder circuit, equipped with active signal modulation. The transponder device is constructed based on microstrip line technology, on a printed circuit board. A integrated signal path switch addresses multiple transmission line terminations, providing the possibility of active backscatter modulation. Incoming radar signals will be re-radiated after the signal modulation, back to the engendering radar transceiver of following motor vehicle. The transported data then provides more reliable identification of other traffic participants.
Due to its small dimensions, this planar circuit design is able to facilitate assembly and commission inside modern motor vehicle setups, than before.

[1] Adaptive Cruise Control
[2] Radio Frequency

Contents

List of Figures

List of Tables

1 Introduction

1.1 Project and Goals

Crash avoidance systems are the most promising development in the research area of traffic safety to prevent or mitigate road accidents. By setting the goal to avoid the crash before it happens, or if that is not possible, to reduce the disruptive effect of the collision, many fields of car crash statistic reports are concerned to profit from these safety assistant developments.
So far, this transponder system only pertains crashes between passenger automobiles, heavy good vehicles and motor cycles. Later on, it can be thought of expanding the application to vulnerable road users, such as pedestrians and cyclists. Therefor, however, the system needs to be improved in terms of alignment independence in direction to the searching radar. This enhanced use though brings along certain other issues and is therefor not considered more closely. If injuries in general, caused by motor vehicle traffic, is taken into account as well, an once again bigger part of preventable casualties in road statistics can be reached.
The European Road Statistic 2008 offers statistics of total fatalities, divided into modes of transport.

Car + Taxi	48.55%
Powered Two-Wheelers	17.88%
Heavy Good Vehicles and Lorries	4.27%
Others[1]	28.87%

Table 1: Fatalities by Mode of Transport [7]

According to this partition, 70.7% of total road fatalities can be affected to profit from the improvements, in best case scenario.
The North American Insurance Institute of Highway Safety (IIHS) released a road statistics report in 2009 [9], assuming Forward Collision Warning Systems (FMC) and Emergency Brake Assist Systems would have been able to prevented 2.1M crashes and 5.8k fatalities that year. Counting only relevant crashes without evidence of braking. The report is based on data from the National Automotive Sampling System General Estimates System (NASS GES) and the Fatality Analysis Reporting System (FARS) in the United States, in years from 2002-2006.
The official statistic reports, provided by the authorities, indicate the notable road safety prospects of cooperating automotive radar systems.

[1] Such as Pedestrians/Cyclists/Agricultural Vehicles

1.2 Automotive Radar Transponder

Transponder systems are able to cooperate with existing radar systems, yet obstructed in motor vehicles. This will lead to expanding those systems, to provide advanced driver assistance systems, by improving crash avoidance capabilities. Collected data is utilized to generate driver warnings and initiate emergency brakes.

Technical advantages of active target identification are:

- Detection
- Tracking
- Pre-Collision Warning Time Span
- Hidden Target Recognition

By halving the traveling speed, kinetic energy is reduced to a fourth, which has a substantial effect on the outcome of car crashes. Pre-collision warning time spans are essential seconds in the respect to decrease velocity, clarifying the facility and need of such systems.
Primary radar systems do not include active target responds. In comparison with those systems, the cooperative transponder increases correct target identification rates.

The following drawing shows a functional diagram of the transponder, operating in the W-Band[1], at 77 GHz.

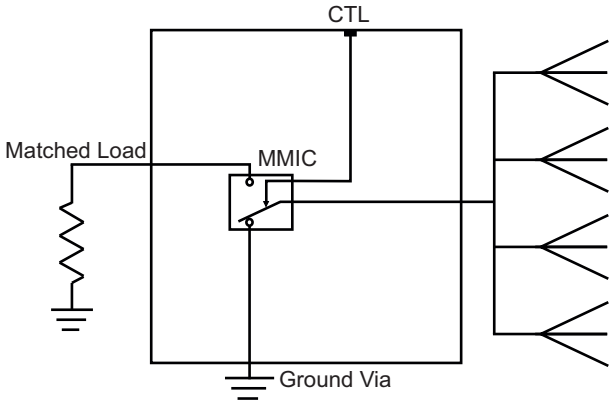

Figure 1: Functional Block Diagram

[1]IEEE U.S. declaration

The transponder works in many ways like today's widespread RFID tags, using modulated backscatter to transmit information. The circuit layout will include four microstrip patch antennas, arranged in a one dimensional antenna array. Mounted in vertically alignment, which is ideal for this kind of car-to-car communication. The beam form is maximum focused in vertical direction and wide ranged in azimuth angles.

Figure 2: Transponder Directivity

Best performance can be gained, when mounted on the backside of a car, at about the same height as the sampling front radar. Directivity pattern of both, radar and transponder, are then optimally utilized.

2 Transponder Theory

2.1 Radar Equations

All kinds of objects of different shapes and materials scatter electromagnetic energy. The principle of passive radar systems is based upon the dependency of re-radiated power density, back at the radar's initial point, and the distance in-between radar and scattering target. When the signal spreads out into air, the power density is strongly attenuating, due to free space loss. About $\sim {}^{1}/_{R^4}$, on growing distance R. As a consequence the signal evaluation must handle very low powered signals, which limits the maximum range in respect to the smallest detectable signal S_{min}.

$$R_{max} = \left[\frac{P_t G_t A_{eff} \sigma}{(4\pi)^2 S_{min}}\right]^{\frac{1}{4}} \tag{2.1.1}$$

For line of sight connection, the radar equation is defined in [15]:

$$P_e = \frac{P_t G_t}{4\pi R^2} \frac{\sigma}{4\pi R^2} \tag{2.1.2}$$

Where P_t is the transmitted power and G_t the antenna gain of the radar transceiver. P_e represents the re-radiated power density, evaluated back at the point of the searching radar. Normally, σ stands for the radar cross section (RCS) of the target. In this case, the transponder only is being considerate as target. Even if it is mounted on the backside of a car, which also contributes to the overall RCS.
Equation 2.1.2 holds for monostatic radar with the same antenna for transmitting and receiving.

The power P_r received by the transponder, is dependent of the antennas effective area A_{eff} and the power density S_i of the incoming electromagnetic waves.

$$P_r = S_i A_{eff} \tag{2.1.3}$$

The effective antenna area depends on the effective patch length L_{eff}. It can be calculated as [5]:

$$L_{eff} = L + 2 \triangle L \tag{2.1.4}$$

The lengths L and $\triangle L$ are described more closely in Section 4.2.

2.1.1 Secondary Radar

The two differences between secondary and primary radar systems, are signal evaluation and signal amplification on side of the target. The second quality forgathers with the fact of a target being known as requested target. This makes it possible to implement features, that improve identification and tracking.
More reliable identification is achieved through implementation of data transport by signal modulation. Tracking can be positively influenced by increasing the transponder's RCS.

Indeed, this thesis is not about an secondary radar transponder, due to the absence of the signal detection and amplification part. The connection to this project is the second quality, the active signal modulation.

2.2 Radar Cross Section

In general, there is no analytic RCS equation for arbitrarily formed objects. [15] defined it as:

$$\sigma = \frac{\text{power reflected toward source/unit solid angle}}{\text{incident power density}/4\pi} = 4\pi R^2 \frac{|E_r|^2}{|E_i|^2} \qquad (2.2.1)$$

For various kinds of targets, the RCS can be approximated with numerical methods, by solving the Maxwell's Equations in simulation. This, however, means considerable effort in order to get good reality compliance.

2.2.1 RCS of Microstrip Antennas

There are two modes of scattering referring to antenna RCS, the *structural mode* and the *antenna mode*.
Taking a closer look on the RCS referring to the structural mode of microstrip patch antennas. The patch itself is of interest and thus equipped with a short circuit termination. No further feeding lines or attachments are added yet. From the radar's point of view, the antenna appears as a metalized patch on the dielectric substrate, with surface size A_{eff}.
Likewise other canonical elements as cubes, cylinders and spheres, a flat plate can

analytically couched in terms of its dimensions and the operating wavelength in free space [8]:

$$\sigma = 4\pi \frac{A_{eff}^2}{\lambda^2} \tag{2.2.2}$$

So far no further circuitry attached to the antennas was concerned. The antenna array, however, needs a feeding structure realized by microstrip lines. These feeding networks will be studied in Section 4.3.
When feeding structures are taken into account, the RCS changes. This is known as the structural mode of antenna scattering. Power, received by the antenna, is transmitted to the feeding lines. The re-radiation of this power then depends on the feeding lines terminating resistance. If the load is matched to the characteristic impedance of the transmission line, all power will be absorbed. Γ_A is the reflection coefficient, showing the reflection ratio between *total reflection* $\Gamma_A = 1$ (short circuit) and *total absorption* $\Gamma_A = 0$ (matched load).

$$\Gamma_A = \tfrac{(Z_A - Z_L)}{(Z_A + Z_L)} \quad 0 \leq \Gamma_A \leq 1 \tag{2.2.3}$$

Z_L is the presumed termination load and Z_A is the antenna radiation resistance. Though, the scattered electric field $E_s(Z_L)$ can be written as:

$$E_s(Z_L) = \underbrace{E_s(Z_L = 0)}_{structural\ mode} - \underbrace{\left[\frac{1}{2} I(0)(1 - \Gamma_A)\right] E_r}_{antenna\ mode} \tag{2.2.4}$$

E_r stands for a radiated field for a unit current excitation [8]. E_r weighted with the reflection coefficient and a current constant, results in the antenna mode part of the equation.
Another consequence of feeding structures is signal attenuation in form of insertion loss of the contained transmission lines and power combiners/splitters. The amount of loss, however, is quite small. Transmission loss of a 50 Ω line on the chosen substrate (Section 3.2) can be estimated as $\ll 0.1\,^{\mathrm{dB}}/_{\mathrm{mm}}$. Calculated with [**?**]. Regarding RF relevant circuit dimensions, of less than 15 mm, it shows small substantial outcome. The second mode of antenna scattering is much more significant. In the literature, different types of scatter mode definitions are introduced. One defines the total backscattered power as structure mode. Others calling it the antenna mode. This paper stays conform with the allocation made by Hansen [10]. Calling the total reflection in short circuit mode, the structural mode. Then subtracting emerging signal attenuation, springing from power absorption, as defined

in Equation (2.2.4). This definition is wider spread than the *matched load definition*, which has quite similar equations [8].

Knott, Shaeffer and Tuley presented patch antenna RCS results with short circuit and matched termination.

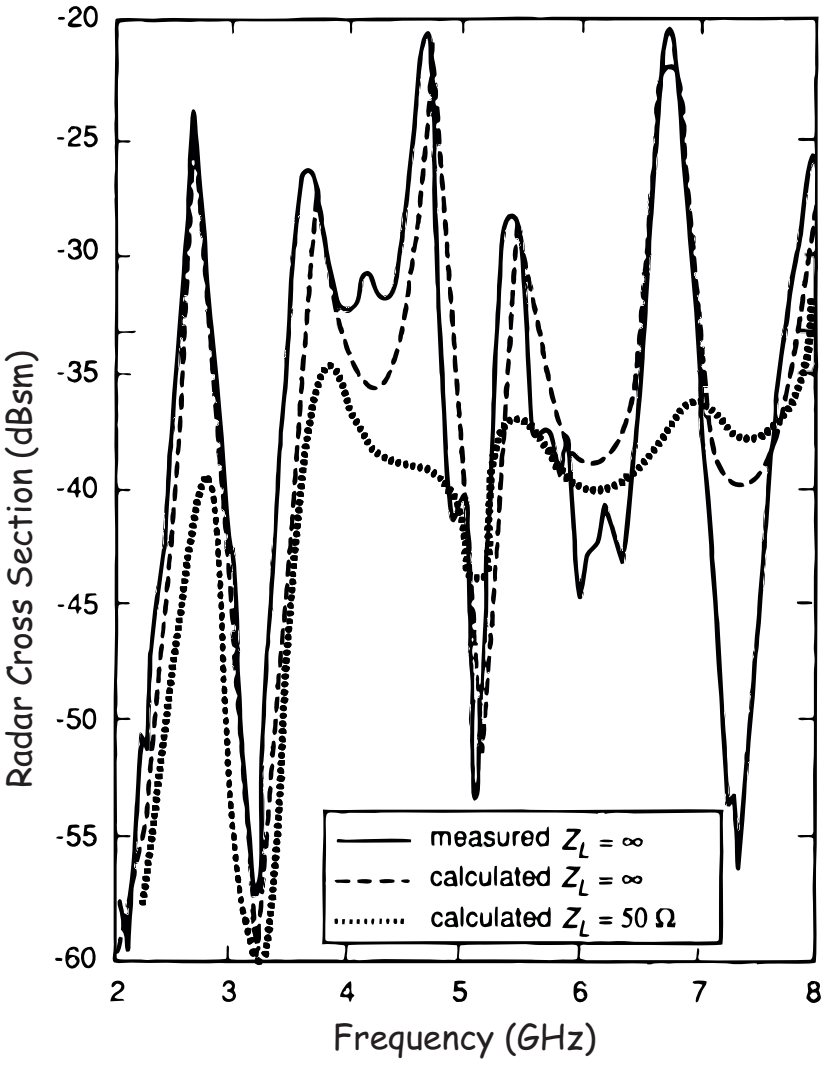

Figure 3: Patch Antenna Scattering Modes [8]

Figure 3 shows two calculations. The first dotted line is open or short circuit, with termination resistance $Z_L \to 0$. The second, shorter dotted line has a matched $50\,\Omega$ termination. With this termination, maxima could be lowered of about 10 to 20 dB. The solid line describes measured RCS, also in short circuit mode. Those results differ from the equivalent ideally calculated dotted line.

The radar cross section is in square units. For that reason, the backscattered power level is in dBsm (decibels relative to a square meter). This data was taken from a corner, probe fed patch antenna, where both x and y modes are excited. Each of the RCS peaks are related to either maximum structural backscatter or self-impedance minimum [8].

2.3 Signal Backscatter Modulation

Information can be modulated on all three describing parameters of an electromagnetic wave. Frequency, amplitude and phase. This holds true for transponder backscatter modulation in general. However, the transponder circuit here includes no active components, which means the two digital modulation schemes ASK [1] and PSK[2] remain possible.
ASK is based on the antenna mode reflection coefficient from Equation (2.2.3). If the antenna is short circuit, the reflection coefficient approximates to 1, where all of the received power is re-radiated. As the load Z_L increases, more power is absorbed. When Z_L exactly matches the transmission line impedance, half of the power will be re-radiated by the antenna and half will be absorbed by the load [16].

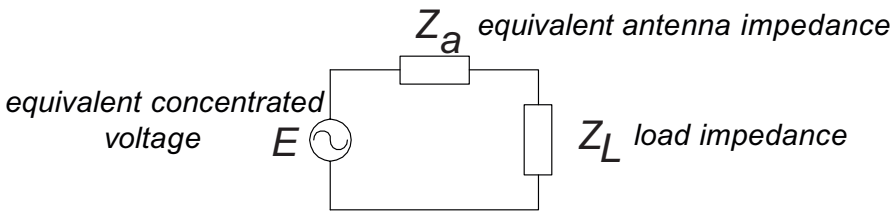

Figure 4: Equivalent Antenna Model and Load Impedance [16]

It is also possible to switch between short circuit and open circuit. In this case, the modulation is PSK. Both terminations have a reflection coefficient close to 1. The phase of the returning signals is different though. The phase distinction of open and short circuit ideally amounts up to 180°.

An ideal transmission line model was assumed for the reflection coefficients, where losses were not considered. Depending on the modulation function and bandwidth, the frequency of the information carrying signal appears as upper and lower side band, allocated around the 77 GHz center frequency peak in the spectrum.

[1] Amplitude Shift Keying
[2] Phase Shift Keying

3 Hardware Considerations

3.1 High Frequency PCB

Today's high frequency circuitries are often based on printed circuit bord (PCB) technology. In order to keep the dimensions small and fabrication costs low. Initial design effort and prototype manufacturing may be higher than other technologies, but for mass production PCBs are faster and cheaper to construct.
Another highly desirable benefit is the possibility to design RF circuits without any lumped elements and therefor possible to manufacture in one lithographic procedure. Thus, no additional soldering needs to be done inside the circuit.
There are many ways to implement transmission lines and waveguides on a PCB, represented in Section 4.1, later in this workout.
Owing to their common use by this time, many different types of transmission lines are well discussed in physical and electrical manner. A standard work in scientific literature is Pozar's Microwave Engineering. [11].

3.2 Dielectric Substrate

In order to pick the right dielectric substrate, where the microstrip line design will be based on, it is necessary to trade-off between best electrical performance and good realizability.
For good radiation behavior and efficiency of the microstrip patch antennas, it is also important to have a rather thick substrate with low dielectric constant ϵ_r [5]. If the thickness increases, however, the width of the microstrip lines increases as well. An undesirable consequence in most cases, since it creates higher production costs and implementation issues.
Balanis [5] states, the circuit bandwidth (BW) is straight proportional to ϵ_r,

$$BW \sim volume^2 \sim \frac{1}{\sqrt{\epsilon}_r} \tag{3.2.1}$$

Achieving greater bandwidth is often of great interest. But then again, the circuitry dimensions diversify in unintended manners. Depending on the application and the demands of disposable BW, circuit dimensions and maximum loss leads to the substrate of best choice.
As dielectric substrate for this transponder, the Rogers RT Duroid 5880 [3] substrate was used. It provides low electrical loss in microstip lines for the dielectric

[2]Volume of the rectangular antenna patch given by $length \times width \times height$

constant $\epsilon_r = 2.2 \pm 0.02 spec.$ [4] and a small dissipation factor $tan\beta = 0.0009$ [4]. The RT 5880 substrate showed good agreement with demands placed in earlier projects, operating around 77 GHz [6].
A lower insertion loss, including radiation in the circuit else than antennas, is important for wireless communication systems, radar and RFID applications, which operate on very low powered signals. This becomes more important, if the physical length of transmission lines increases.

The next important characteristic substrate value is the height d of the dielectric material. As this defines the W/d ratio, where W is the width of the transmission line. The W/d ratio is liable for the characteristic impedance of transmission lines.

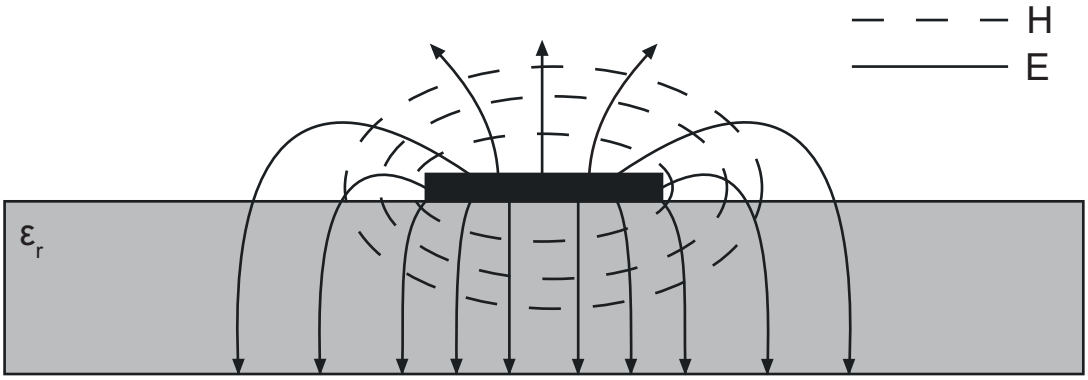

Figure 5: Microstrip Transmission Line Fields

Forward-looking to the manufacturing, the width of printed waveguides is required to be above a minimum precept, depending on the producers capabilities. At the time of this project, the lowest diameter of printed conductors, available on the market, was down to 50 μm. If the width is a fixed required size and assuming the layout to be based on 50 Ω system, the substrate's height d is the parameter in charge of fulfilling these conditions. A 50 Ω system means that all external ports and crossings have the characteristic impedance of 50 Ω. On the downside, this does not mean there are no other impedances in the circuitry. There might be different characteristic impedances of transmission lines when it comes to power dividers, wavelength transformer and other parts of the matching network, discussed in Section 4.3. Unfortunately, higher impedances means smaller transmission line dimensions. It is important to make sure, that those dimensions fit the smallest printable width.

The chosen thickness of the dielectric material in the substrate was 0.254 mm, with a 17 μm copper cladding.

Having in mind designing a future viable product, based on this prototype, further properties of Rogers 5880 substrate might be advantageous as well. Counting low moister absorption, semi flexible or good handling in cutting and machining. [3] Those reasons and the overall flat appearence make PCB a widely used technology for high frequency automotive purposes nowadays.

4 Transponder Circuit Design

Note: Equations concerning project related variables are highlighted in boxes.

Practical design calculation equations are taken from Antenna Theory [5], by Balanis.

4.1 Microstrip Lines

Microstrip transmission lines are two dimensional transmission lines. They can be formed by lithographic or laser technology. On the contrary to striplines, microstrips are not fully coated by dielectric material, but applied onto single layered substrates. Other representatives of printed transmission lines are coplanar transmission lines and printed slotline waveguides. Coplanar waveguides have the ground reference on the same surface as the transmitting waveguide. While slotlines appear as the opposite design to microstrip, but differ in electromagnetic field distribution.

Figure 6 shows the electric and magnetic field, spreading out over two different dielectric materials. On the one hand, inside the substrate, prevailed by the dielectric constant ϵ_r. In this case $\epsilon_r = 2.2$. On the other hand occupying free space above the transmission line. This makes a microstrip line an inhomogeneous waveguide. Complicating the analysis of its electromagnetic properties.
Due to the different phase velocities in substrate and air, calculated by

$$v = \frac{c}{\sqrt{\epsilon_r}} \tag{4.1.1}$$

a TEM propagation mode is not possible. c is the velocity of light and the approximative phase velocity in air at the same time. A quasi TEM-mode with a hybrid TM-TE wave appears instead of a pure TEM propagation mode, thanks to a very thin dielectric substrate, compared to the wavelength ($d \ll \lambda_c$) [**?**]. Assuming an operating frequency f_c.

Microstrip transmission lines can be modulated in an equivalent lumped element model.

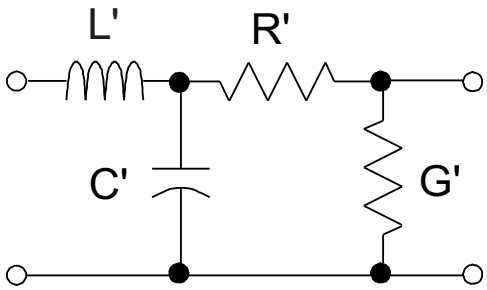

Figure 6: Lumped Element Transmission Line Model [2]

The four lumped elements in this model,

R'	series resistance in $[\Omega/m]$
G'	series conductance $[H/m]$
L'	shunt conductance $[S/m]$
C'	shunt capacitance $[F/m]$

represent the transmission line coatings, normalized per unit of length.

While R descends from the finite conductivity of the conductor material. G represents the losses due to the dielectric material. The shunt conductance L is the self-inductance of the transmission line and the ground reference. The shunt capacitance originate from the proximity of the two conductor layers on top and underneath the dielectric material. [**?**]

4.1.1 Impedance Matching

The complex characteristic impedance Z_0 is given by the equation of:

$$Z_0 = \sqrt{\frac{R' + j\omega L'}{G' + j\omega C'}} \tag{4.1.2}$$

As already mentioned, microstrip lines are inhomogeneous waveguides and thus the characteristic impedance can not be analytically calculated. Again, in terms of $d \ll \lambda_c$, it can be assumed to find a *quasi-static approximation* [14]. That means it is presumed, that a quasi-TEM mode is propagating as described in Section 4.1. Using this approximation, the wave impedance results in:

$$Z_0 = \frac{1}{c}\sqrt{CC'} \tag{4.1.3}$$

Where C is the capacitance (per unit of length), if the substrate gap d hypothetical being free space instead of dielectric material. Certainly, in practical terms neither Equation (4.1.2), nor (4.1.3) are applicable. Shunt capacities, conductances or impedances are unknown values. Z_0 needs to be characterized by available parameters like ϵ_{eff} and W/d ratio. An approximative calculation for microstrip lines is presented in [**?**].

$$Z_0 = \begin{cases} \dfrac{60}{\sqrt{\epsilon_{eff}}} \ln\left(\dfrac{8d}{W} + \dfrac{W}{4d}\right) & \text{for } W/d \leq 1 \\ \dfrac{120\pi}{\sqrt{\epsilon_{eff}}\left[\frac{W}{d} + 1.393 + 0.667 \ln\left(\frac{W}{d} + 1.444\right)\right]} & \text{for } W/d \geq 1 \end{cases} \tag{4.1.4}$$

W represents the width of the transmission line. The characteristic impedance is the most important quality in an the transmission line design, when it comes to feeding networks (Section 4.3). A mismatched wave impedance degrades the performance of a high frequency application.
Important issues in this context are summarized by Pozar [**?**], revealing the benefits as:

- Maximum power delivery to matched loads
- Minimum power loss in feed line
- Improving the Signal to Noise Ratio (SNR) for impedance sensitive components[1]
- Reducing *amplitude and phase errors*[2] in power distributing networks, such as antenna feeding arrays

By means of Equation (4.1.4), a yet determined substrate height and given values of the transmission line conductance (coating per unit of length), it is now possible to calculate the width of a $50\,\Omega$ line. W was calculated with *ADS LineCalc*[3] and optimized in *ADS Schematic*[3].

[1] E.g. Antennas
[2] Evident from S-Parameters
[3]

$$W = 0.790 \text{ mm}$$

with

$$W/d = \frac{0.790\,\text{mm}}{0.254\,\text{mm}} = 3.11$$

Those results may then be aligned with the minimum width condition from Section 3.2.

4.2 Rectangular Patch Antenna

In order to get best application functionality, a solicitous antenna design is of great significance. Vital for radiation performance and pattern and also impedance matching, the patch antenna parameter must be calculated precisely. Rectangular microstrip patch antenna equations are well studied and documented for those reasons.
A lot of patch antenna feeding structures exist, in terms of electro-magnetic coupling (e.g. aperture-coupled, proximity-coupled).
Patch antennas can also be fed by a probe going through the substrate onto the ground plate. The disadvantages are more complicated structures and thicker substrates. Thus microstrip antennas are often fed by microstrip feeding lines. As well, as it has been chosen in this project.

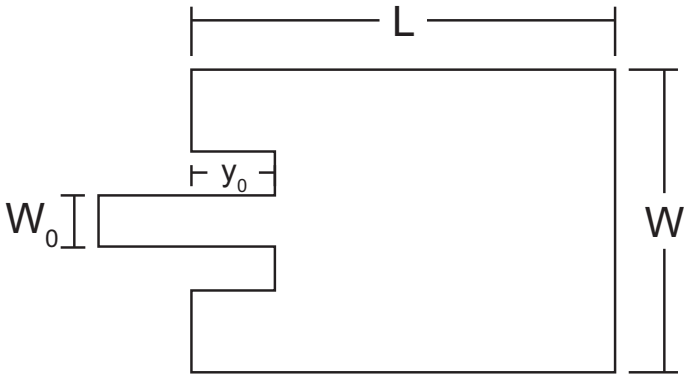

Figure 7: Rectangular Patch Antenna [5]

The physical patch design parameters from Figure 7 are determined, using the *transmission line model*, where all electrical parts on the top of the substrate and

its field distribution are assumed to be in a homogeneous environment, with an dielectric constant ϵ_{eff}, instead of two separated parts filled with ϵ_r and air. This makes the model less accurate as the *cavity* or *full wave model* [5], but facilitates the analysis severely.

Design origin parameters in this project have been stated as:

Resonant Frequency	77	[GHz]
Desired Resonant Input Resistance	100	[Ω]
Substrate Height	0.254	[mm]
Dielectric Constant	2.2	

Table 2: Design Origin Parameters

First, calculating the physical width W of the patch.

$$\begin{aligned} W &= \frac{c_0}{2f_r}\sqrt{\frac{2}{\epsilon_r+1}} \\ &= \frac{3\times 10^8}{2\cdot 77\times 10^9}\sqrt{\frac{2}{2.2+1}} \\ &= 1.540\,\text{mm} \end{aligned} \tag{4.2.1}$$

Since W does not affect the resonance frequency of the first mode, TM_{010}, which is a function of the physical patch length L. It does, however, influence the radiation efficiency by the effective dielectric constant [5]. Eventually the width must be great enough to provide good impedance matching capability, but small enough to eliminate higher order modes and providing better radiation efficiency and lower dielectric loss. For

$$\lim_{W\to\infty}\epsilon_{eff} = \epsilon_r \quad 1 < \epsilon_{eff} < \epsilon_r \tag{4.2.2}$$

ϵ_{eff} is determined under the impression of $W/d > 1$:

$$\begin{aligned}\epsilon_{eff} &= \frac{\epsilon_r + 1}{2} + \frac{\epsilon_r - 1}{2}\left[1 + 12\frac{h}{W}\right]^{-1/2} \\ &= \frac{2.2 + 1}{2} + \frac{2.2 - 1}{2}\left[1 + 12\frac{0.254}{0.154}\right]^{-1/2} \\ &= 1.948\end{aligned} \tag{4.2.3}$$

Two radiating slots separated by the length L cause the electrical length to be longer, because of fringing effects on the rims of the patch. As a result the actual physical length is given by:

Extended Length

$$\begin{aligned}\triangle L &= d \cdot 0.412\frac{1.948 + 0.3)\left(\frac{W}{d} + 0.264\right)}{(\epsilon_{eff} - 0.258)\left(\frac{W}{d} + 0.8\right)} \\ &= d \cdot 0.412\frac{(1.948 + 0.3)\left(\frac{1.540}{0.254} + 0.264\right)}{(\epsilon_{eff} - 0.258)\left(\frac{1.540}{0.254} + 0.8\right)} \\ &= 0.120\,\text{mm}\end{aligned} \tag{4.2.4}$$

Physical Length

$$\begin{aligned}L &= \frac{\lambda}{2} - 2 \triangle L \\ &= \frac{3 \times 10^8}{2 \cdot 77 \times 10^9\sqrt{1.948}} - 2 \cdot 0.120 \\ &= 1.156\,\text{mm}\end{aligned} \tag{4.2.5}$$

The following results are calculated with the method of moments (MoM). This numerical computational method transforms the partial differential field equations problem into a approximative linear system of coefficient matrices with a finite number of entries [13].
The S_{11} data in dB magnitude describes the return loss, starting from the antenna feeding point. S_{11} below -10 dB is known to be good [?]. -15 dB represent $\approx$ 3% of returning power.

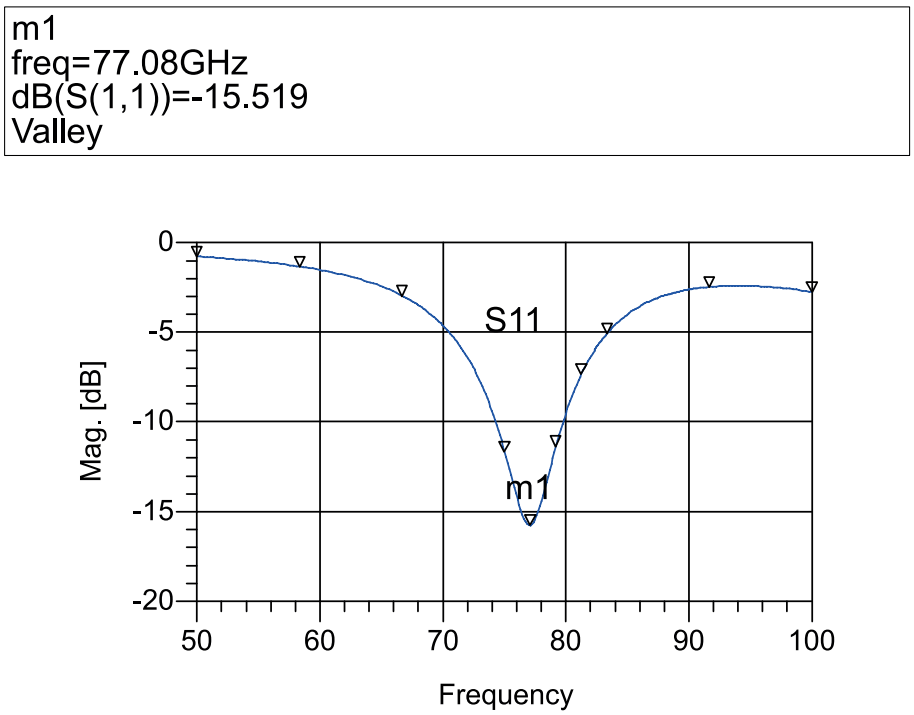

Figure 8: Antenna S-Parameter

Figure 9 shows the antenna gain, compared to an isotropic radiator. The range patch antenna directivity is about 7-9 dB [?]. In this case, 8.093 dB was reached in vertical radiation direction.

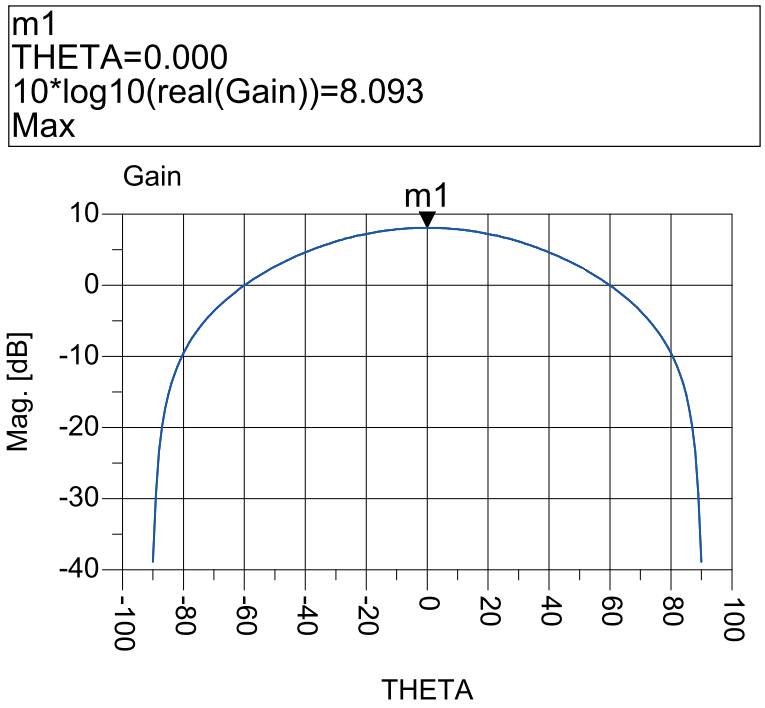

Figure 9: Antenna Gain

4.3 Feeding Network

Feeding networks for patch antenna arrays are either series-feed networks[1] or corporate-feed networks[2]. In this instance, no special polarization or beam forming scanning ability must be achieved, so the two feeding networks are equally eligible. Although corporate feeding have more isolated paths to the antennas and therefore each of the feeding lines has less impact on the whole feeding structure, regarding attenuation and reflection. [5] Corporate feeding is more convenient and picked for this project.
Mutual coupling can be kept low, by leaving adequate distance between the radiating antennas. This means maintaining gaps greater than $\lambda/2$.

Transitions lines merge the 100 Ω feeding points of the antennas to one 50 Ω feeding point for the entire array. This is illustrated in the drawing of figure 10. Starting from 50 Ω input resistance, at the lower feeding point, the network spreads out into two 100 Ω transmission lines. Before the next split, the line impedance needs to be

[1] one transmission line feeding multiple antennas in a series assembly
[2] transmission line splitting into multiple separate feeding lines, using power splits

transformed again into 50 Ω. The transition is achieved by a $\lambda/4$ transformation, between one hundred and fifty ohms.

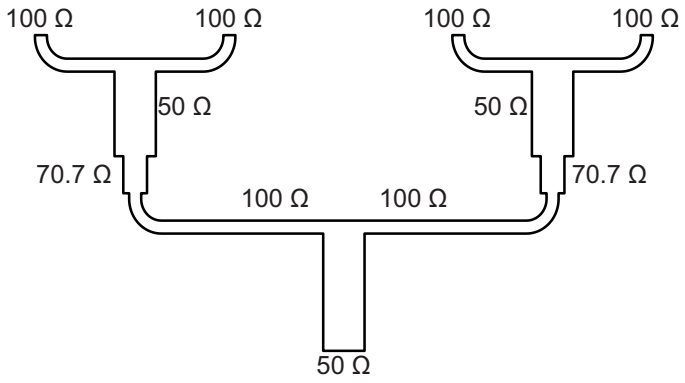

Figure 10: Feeding Network

Another important issue, when designing a feeding network, is to prevent undesired radiation at transmission line discontinuities inside the network. Concerning curves of microstrip lines, radiation can be mitigate by choosing grater radii.
The overall transponder layout is presented in Figure 11

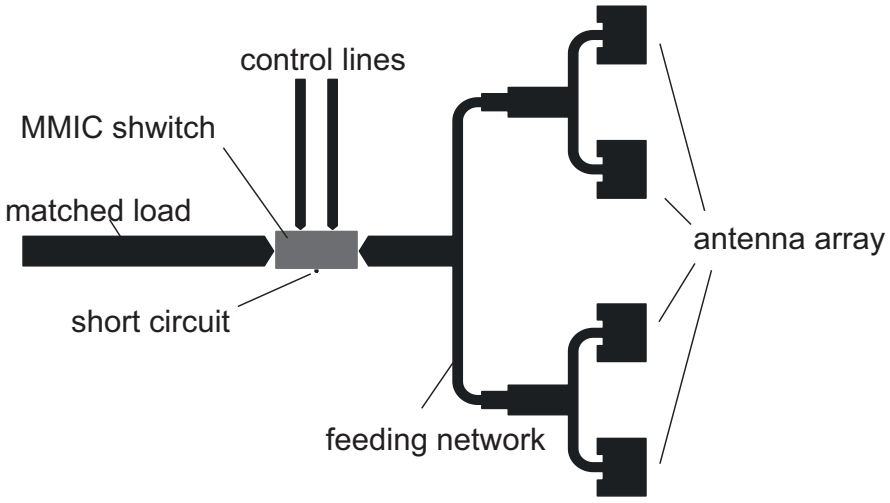

Figure 11: Transponder Overview

4.4 Simulation Results

Figures 12 to 15 provide calculated results of the antenna array and the attached feeding network.

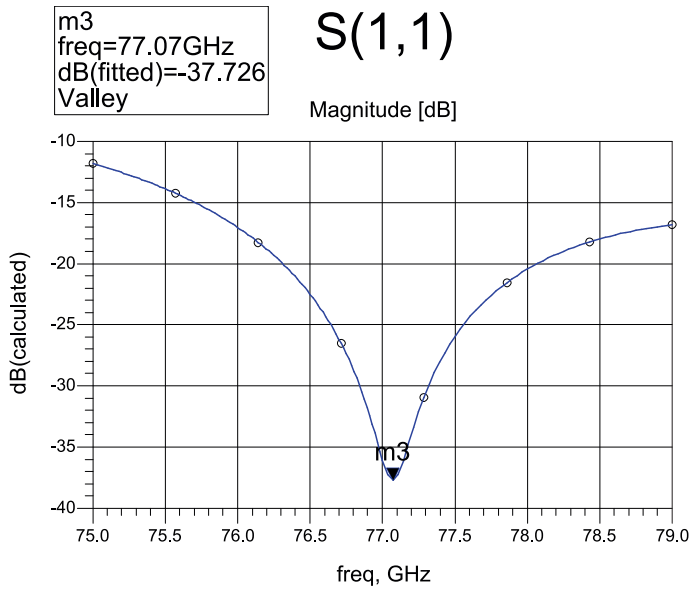

Figure 12: S-Parameter oh the Final Transponder Circuit

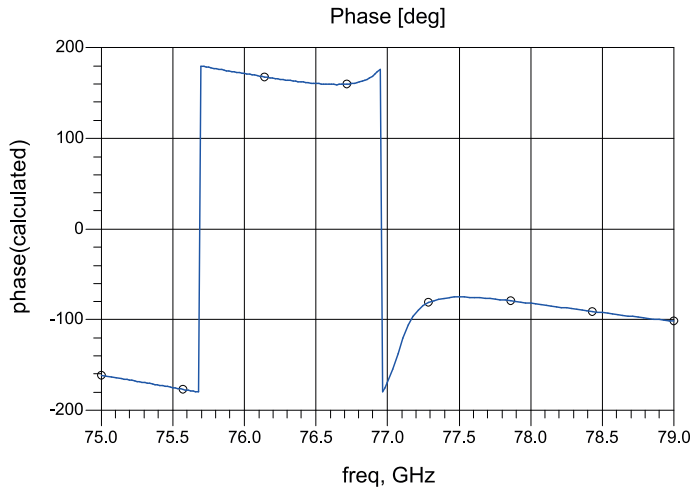

Figure 13: Phase over Frequency

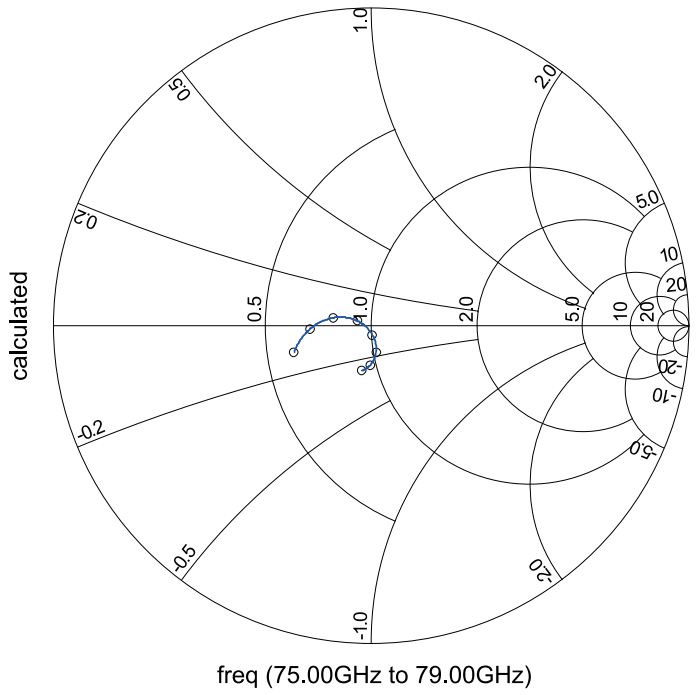

Figure 14: Smith Diagram

With a resumed radiation directivity pattern of four patch antennas, visualized from 90° angle and directed in $\phi = 90°$ elevation radiation:

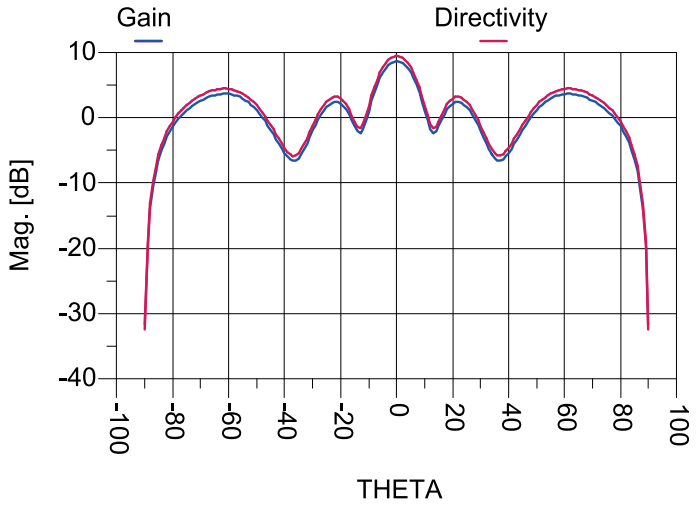

Figure 15: Radiation Directivity

5 Fabrication

In theory and simulation, designing applications in this field of ultra high frequency at the W-Band may work through right properly. Even though, there are not many similar papers or projects available to rely on. The quantity of RF application decreases on rising frequency. One of the reasons is the squaring free space loss on growing frequencies, especially for communication systems. For a lot of materials, manufacturing routines and components merely declarations for lower frequencies exists, with deficient statements about their ultra high frequency suitability.

5.1 Fabrication Requirements

As it has been already pointed out, fabrication requirements have to be preliminary considerate in the beginning of design work. Those requirements mostly demand minimum dimensions or height and clearance regimentations for successfully accomplishing manufacturing steps. Owing to the limited physically accuracy of producing machines or material limitations.
Including external circuit parts, such as MMIC chips, it is necessary to match the mounting and bonding requirements, as well.

5.2 MMIC Mounting and Bonding

Lumped elements are mostly unsuitable for ultra high frequency applications. This is because of its inapplicable RF qualities at growing frequencies. Parasitic impedances and capacitances grow stronger in relevance. Linear element behavior must be checked for frequency dependency then as well [12]. Circuit parts, which are normally realized by lumped elements, such as diodes, resistors and capacities, often can be replaced by integrated MMIC chips.
In this work the aforementioned GaAs PIN diode based SPDT MMIC, HMC-SDD 112-SX chip [1] from Hittite, was used to provide signal path switching. Single Pull Double Throw (SPDT) means one input port and two output ports of the switch. MMIC stands for Monolithic Microwave Integrated Circuit.
Practically, there are two ways to connect the chip into the PCB environment. First, if the circuit is based on coplanar technology, with defined ground on the upper side of the substrate, the MMIC can be mounted right on top of the dielectric surface. The signal path must be electrically connected to the rest of the circuits transmission lines, but also to the ground reference. Although, in theory, height differences and extra bonding wires could evoke practically implementation

problems.
If the transponder is not in coplanar design, however, the chip requires ground contact on its bottom side. Recommended by manufacturer Hittite, the chip then needs to be mounted to about the same height of the substrate surface:

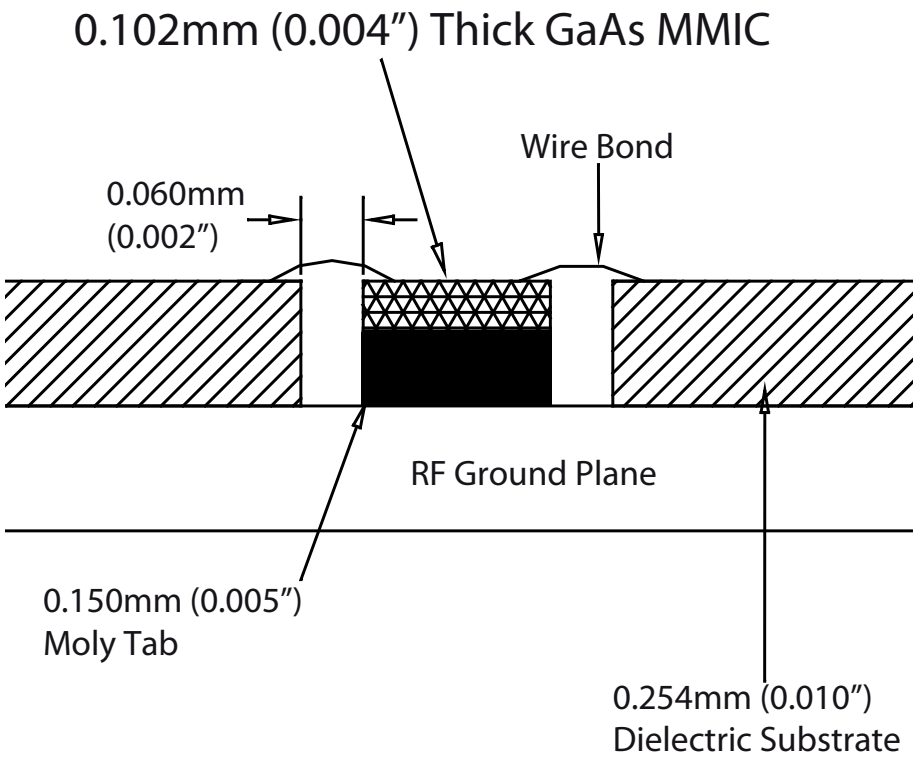

Figure 16: MMIC Mounting and Bonding [1]

Figure 16 reveals very small physical spaces in height and width, causing practical problems in building a prototype. This leaves little margin for production inaccuracy. With no possibility to mill on to the downside ground plate, which is about 17μm thick, the moly tap has to be galvanic coupled to the ground copper cladding. This connection must handle electronic and physic requests.

5.3 Practical Problems

In this thesis an automotive radar transponder prototype was designed and fabricated. The small microstrip line dimensions complicates finding manufacturing partners for the lithographic circuit production. Another problem was to mount

the MMIC chip on the moly tap and to place it inside the substrate, by hand. For volume production, a permanent stable ground plate would be essential, as well as automated soldering machines, which are accurate to the micrometer.
Recommended for continuing projects are coplanar composition. As well as preventing the mounting problems attained with all integrated, non monolithic switching circuitry, on the same substrate.

6 Measurement and Results

6.1 Test Setup

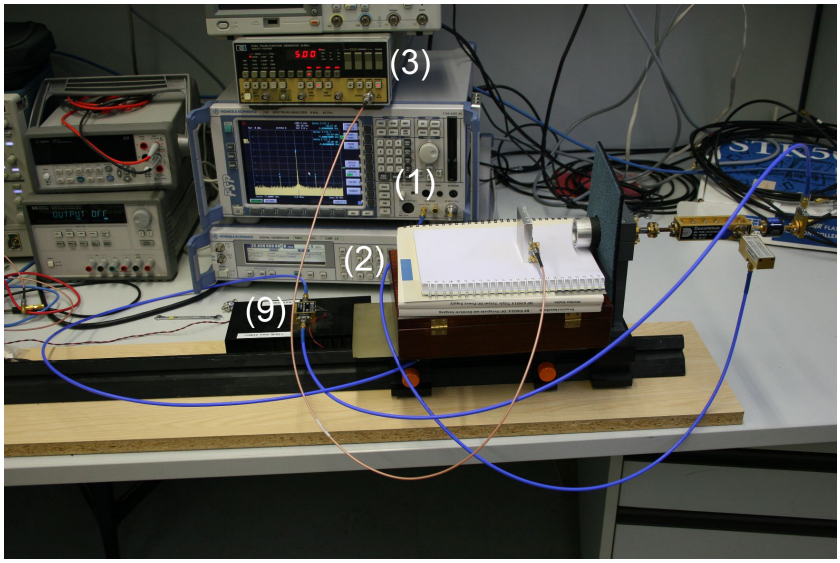

Figure 17: Measurement Laboratory Setup - Front View

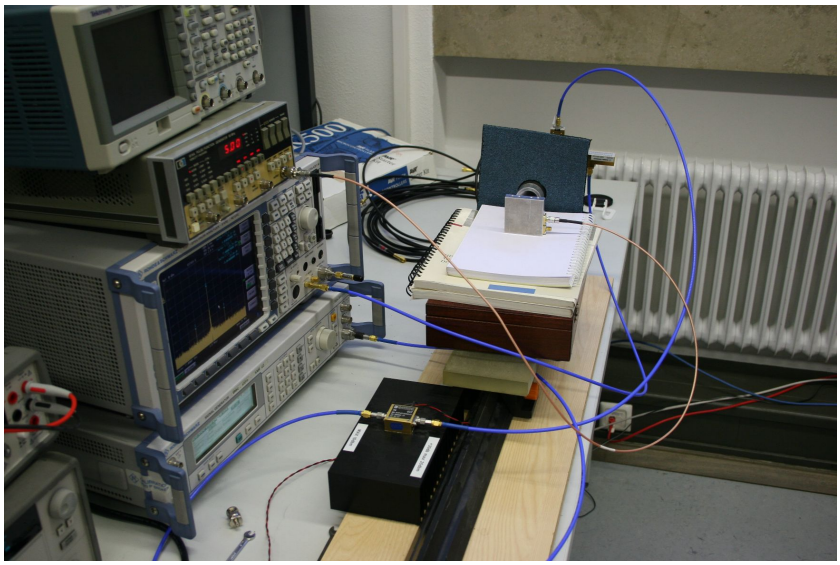

Figure 18: Measurement Laboratory Setup - Side View

The mesurement setup for the transponder function tests is shown in Figures 17 and 18. Measurement equipment and used RF components are listed in Table 3 and 4.

Device	**Fabricator**	**Typ**	#
Spectrum Analyzer	Rohde & Schwarz	FSP	1
Signal Generator	Rohde & Schwarz	SMR-40	2
Signal Pulse/Function Generator	HP	8116A	3

Table 3: Measurement Devices

Component	**Fabricator**	**Typ**	#
Passive Frequency Multiplier	Ducommun	FMP-KF312-01	4
Faraday Isolator	Ducommun	FFF-12-01	5
Directional Coupler	Ducommun	PCM-120330HB-01	6
Waveguide Converter	Ducommun	PRC-10094-01	7
Beam Antenna	NA	NA	8
Amplifier	Ducommun	AHP-25102530-01	9
Mixer	Rohde & Schwarz	FS-Z90	10

Table 4: Additional Setup Components

The signal generator (2) operates in a frequency range of 10 MHz - 40 GHz. The spectrum analyzer (1) is capable to evaluate frequencies up to 40 GHz. A passive frequency multiplier (4 in Figure 19) triples its input frequency, in order to get the 77 GHz transmitting (TX) signal. $25.\bar{6}\,\text{GHz} \times 3 \simeq 77\,\text{GHz}$
The $25.\bar{6}$ GHz signal (exact up to ten digits) is generated and emitted at 0 dBm output power and straight reinforced with an amplifier. In linear behavior, the amplifier (9) lifts its output power about +30 dB, in respect to the input power. The signal is then transmitted to the frequency multiplier (5) and a downstream one-way isolator (5). This Faraday Isolator prevents power from coupling back into the signal generators output port. A directional coupler transports the TX signal through a rectangle to sphere waveguide converter into the directed antenna (8).

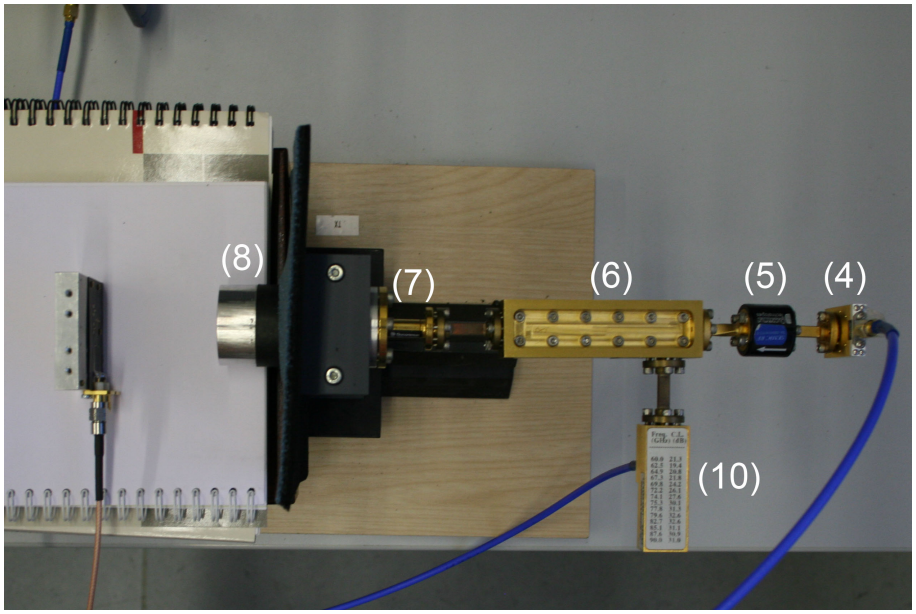

Figure 19: TX/RX Signal Path - Transponder - Setup

After traveling the clearance in between, the emitted waves hit the antenna array of the transponder. The transmitter re-radiates the received electromagnetic waves, after the signal modulation is done (Section 2.3). The directional coupler (6) leads the RX signal to the mixer junction (10), where it is mixed down to suit the possible receiving frequency range of the spectrum analyzer. It is therefor connected to the spectrum analyzer's external LO input port.

6.2 Results

In the following, measurement results of the PSK modulated transponder signal are presented. The transponder was installed in close proximity to the beam antenna, about 0 cm - 5 cm. Wider gaps did not show applicable results, due to insufficient adjustment means and the strong directivity of the sphere antenna.
The spectrum in Figure 20 originates from a 10 MHz binary phase shift keying modulation. The rectangle modulation signal is provided by the signal function generator (3) and connected via SMA connector to the fist control signal input port of the switch.
Markers show the returning power level (dBm) and the value of the center frequency peak and the mixed multiple side peaks, in GHz.

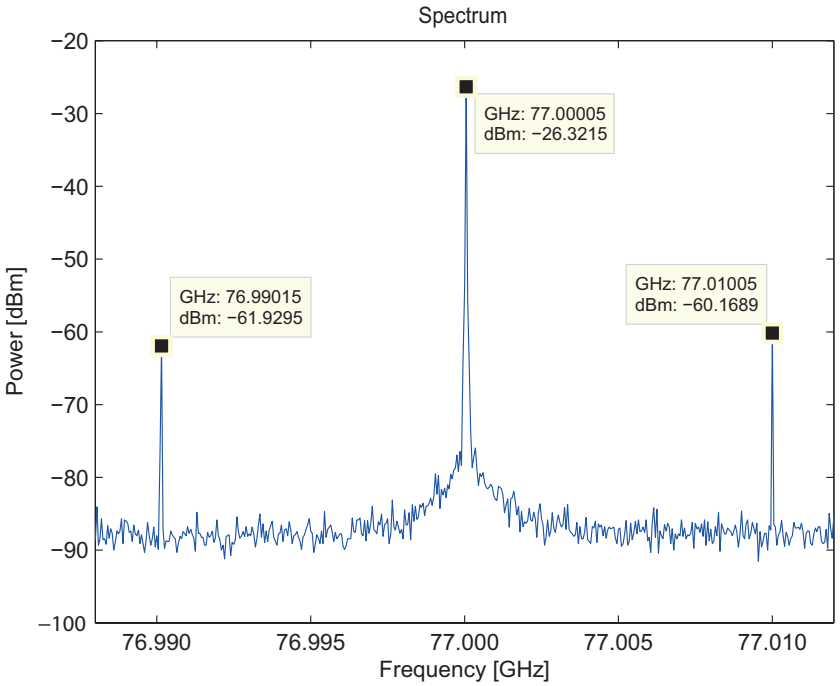

Figure 20: 10 MHz PSK

The power level difference between the ∼ -26 dBm carrier frequency peak and the ∼ -60 dBm side peaks is about 34 dB. Reasons for this are insertion loss at antenna and transmission, impedance mismatches and manufacture inaccuracies. In particular the assembly of the bonding wires between waveguide and switch pads is dominated by imprecisions, which causes manufacture guidelines hardly being met.

Figure 21 also shows PSK referring to 2 MHz modulation, on a wider frequency range, including multiple side peaks.

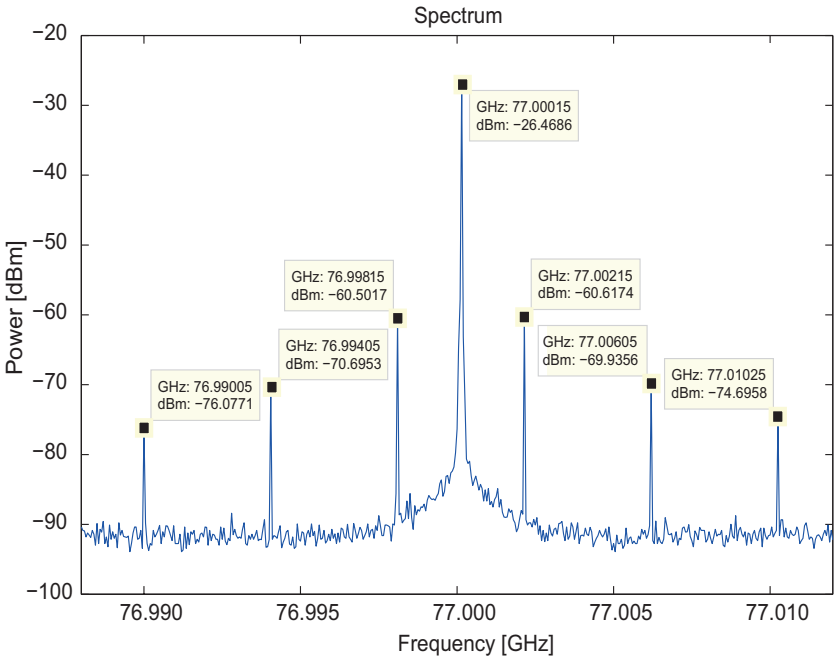

Figure 21: 2 MHz PSK

Increasing the power level of the modulated signal must be the main target in continuing projects. For commercial products, identification reliability will be vital and the most important property. In practical terms a maximum signal strength is desirable. Multi-path propagation, attenuation and signal noise proved dominating character in practice.
For transponders, permanently installed at the backside of motor vehicles, active signal amplification could be the best way to bypass this problem.
Signal amplification, however, might not be an option for pedestrian protection in form of small mobile devices. Another benefit of active radar transponder is signal evaluation. Front vehicles may use the receiving radar signals to generate rear crash warnings.

7 Conclusion

This bachelor's thesis was about designing a 77 GHz radar transponder and brining it into operation. The goal was to construct a small but affective transponder for automotive purposes. To improve and expand today's driving assistant systems in adaptive cruise control. The challenge was to built a small dimensional transponder on PCB technology, without any additional signal amplification, for more convenient integration in present systems.

At first, the functional principle of the transponder were outlined. Primarily considerations on materials, layout and construction were made.

In the next step, the PCB layout was constructed and simulated in *ADS Schematic* and *ADS Momentum*. Excellent simulation results increase the chance of success in hardware layout. Therefor the effort in simulation process was quite considerable.

In order to realize the transponder circuit in hardware, production problems had to be faced. Ultra high frequency application, like this, need competent manufacturing partners and suppliers with practical experience in this field.

Finally the transponder was manufactured properly and good test results were achieved. Based on the obtained results of the prototype, certain problems can be faced more detailed. Hopefully leading to high-performing automobile transponder with highly effective pre-crash warnings systems.

References

[1] Hittite microwave corporation. http://www.hittite.com/content/documents/data_sheet/hmc-sdd112.pdf.

[2] Microwaves101.com. http://www.microwaves101.com/content/downloads.cfm, 2011.

[3] Rogers corporation. http://www.rogerscorp.com/acm/products/10/RT-duroid-5870-5880-5880LZ-High-Frequency-Laminates.aspx, 2011.

[4] Rogers corporation. http://www.rogerscorp.com/documents/606/acm/RT-duroid-5870-5880-Data-Sheet.aspx, 2011.

[5] Constantine A. Balanis. *Antenna Theory.* John Wiley & Sons, Inc., third edition, 2005.

[6] Steven S. Gearhart Bradley G. Porter. 77 ghz dual polarized slot-coupled patches on duroid with teflon lenses for automotive radar systems. 1998.

[7] José Luiz Diez Christophe Nicodème, Konstandinos Diamandouros. European road statistics 2010. http://www.erf.be/images/stories/Statistics/2010/ERF_European_Road_Statistics_2010.pdf, 2010.

[8] Michael T. Tuley Eugene F. Knott, John F. Shaeffer. *Radar Cross Section.* Scitech Publishing, Inc., second edition, 2004.

[9] Charles M. Farmer. Crash avoidance potential of five vehicle technologies. http://www.iihs.org/research/topics/pdf/r1107.pdf, 2008.

[10] R. C. Hansen. *Relationships Between Antennas as Scatterers and as Radiators*, volume 77. Proceedings of the IEEE, 1989.

[11] David M. Pozar. *Microwave Engineering.* John Wiley & Sons, Inc., third edition, 2005.

[12] Mihaela Radulescu. Predicted behaviour of lumped elements at frequencies¿10ghz. http://www.usmicrowaves.com/appnotes/usm_an_103_behavior_of_lumped_elements.htm, 2009.

[13] W.D. Rawle. The method of moments: A numerical technique for wire antenna design. http://highfrequencyelectronics.com/Archives/Feb06/HFE0206_Rawle.pdf, 2006.

[14] Peter Russer. *Electromagnetics, Microwave Circuit And Antenna Design For Communications Engineering.* Artech House, Inc., second edition, 2006.

[15] Merrill I. Skolnik. *Introduction to Radar Systems*. McGraw-Hill, third edition, 2001.

[16] Chris Turner. Backscatter modulation of impedance modulated rfid tags. `www.rfip.eu/downloads/backscatter_tag_link_budget_and_modulation_at_reader_receiver.pdf`, 2003.